HHS Public Access

Author manuscript

Eur J Pharmacol. Author manuscript; available in PMC 2018 January 05.

Published in final edited form as:

Eur J Pharmacol. 2017 January 05; 794: 115–126. doi:10.1016/j.ejphar.2016.11.026.

Pharmacological studies on the NOP and opioid receptor agonist PWT2-[Dmt¹]N/OFQ(1-13)

Maria Camilla Cerlesi[1], **Huiping Ding**[2], **Mark F Bird**[3], **Norikazu Kiguchi**[2], **Federica Ferrari**[1], **Davide Malfacini**[1], **Anna Rizzi**[1], **Chiara Ruzza**[1], **David G Lambert**[3], **Mei-Chuan Ko**[2], **Girolamo Calo'**[1,*], and **Remo Guerrini**[4]

[1]Section of Pharmacology, Department of Medical Sciences, and National Institute of Neurosciences, University of Ferrara, Italy

[2]Department of Physiology & Pharmacology, Wake Forest University School of Medicine, Winston-Salem, North Carolina, U.S.A.

[3]Department of Cardiovascular Sciences, University of Leicester, Division of Anaesthesia, Critical Care and Pain Management, Leicester Royal Infirmary, Leicester, LE2 7LX. UK

[4]Department of Chemical and Pharmaceutical Sciences and LTTA, University of Ferrara, Italy

Abstract

An innovative chemical strategy named peptide welding technology (PWT) has been developed for the facile synthesis of tetrabranched peptides. [Dmt[1]]N/OFQ(1-13)-NH_2 acts as a universal agonist for nociceptin/orphanin FQ (N/OFQ) and classical opioid receptors. The present study investigated the pharmacological profile of the PWT derivative of [Dmt[1]]N/OFQ(1-13)NH_2 (PWT2-[Dmt[1]]) in several assays in vitro and in vivo after spinal administration in monkeys subjected to the tail withdrawal assay. PWT2-[Dmt[1]] mimicked the effects of [Dmt[1]]N/OFQ(1-13)-NH_2 displaying full agonist activity, similar affinity/potency and selectivity at human recombinant N/OFQ (NOP) and opioid receptors in receptor binding, stimulation of [^{35}S]GTPγS binding, calcium mobilization in cells expressing chimeric G proteins, and BRET studies for measuring receptor/G-protein and receptor/β-arrestin 2 interaction. In vivo in monkeys PWT2-[Dmt[1]] elicited dose-dependent and robust antinociceptive effects being more potent and longer lasting than [Dmt[1]]N/OFQ(1-13)-NH_2. The analgesic action of PWT2-[Dmt[1]] was sensitive to the NOP receptor antagonist J-113397, but not naltrexone. Thus, the present study demonstrated that the tetrabranched derivative of [Dmt[1]]N/OFQ(1-13)-NH_2 obtained with the PWT technology maintains the in vitro pharmacological profile of the parent peptide but displays higher potency and longer lasting action in vivo.

*Corresponding author: Department of Medical Sciences Section of Pharmacology University of Ferrara via Fossato di Mortara 19 44121, Ferrara, Italy.

Author contributions:

RG, GC, DGL, and MCK designed research; MCC, HD, MFB, NK, FF, DM, AR, and CR performed research and analyzed data; RG contributed unpublished reagents/analytic tools; MCC, DGL, MCK, RG and GC wrote the paper.

Keywords

PWT2-[Dmt[1]]N/OFQ(1-13); NOP and opioid receptors; receptor binding; stimulation of [^{35}S]GTPγS binding; calcium mobilization; monkey spinal analgesia

1. Introduction

Recently an innovative chemical strategy for the facile synthesis of tetrabranched peptide derivatives has been developed and named peptide welding technology (PWT) (Guerrini et al., 2014). The PWT has been applied to different peptide sequences including nociceptin/orphanin FQ (N/OFQ) (Rizzi et al., 2014; Rizzi et al., 2015), neuropeptide S (Ruzza et al., 2015), and tachykinins (substance P, neurokinin A and B) (Ruzza et al., 2014). These studies demonstrated that PWT derivatives maintained the in vitro pharmacological profile (pharmacological activity, potency and selectivity of action) of the parent peptide sequences while showing higher in vivo potency and particularly long lasting action.

Previous studies demonstrated that [Dmt[1]]N/OFQ(1-13)-NH_2 behaves as a universal agonist for N/OFQ (NOP) and classical opioid receptors (Molinari et al., 2013). In particular, the mixed NOP/opioid full agonist activity and high affinity/potency of [Dmt[1]]N/OFQ(1-13)-NH_2 was demonstrated at human recombinant receptors in receptor binding, calcium mobilization and [^{35}S]GTPγS binding studies, at rat spinal cord receptors in [^{35}S]GTPγS binding experiments and at guinea pig receptors inhibiting neurogenic contractions in the ileum. Moreover in vivo in the tail withdrawal assay in monkeys [Dmt[1]]N/OFQ(1-13)-NH_2 given intrathecally (i.t.) elicited robust and long-lasting antinociceptive effects (Molinari et al., 2013).

Thus, the purpose of the present study was to investigate the pharmacological profile of the PWT derivative of [Dmt[1]]N/OFQ(1-13)-NH_2 (PWT2-[Dmt[1]] see Fig. 1 for chemical structure). The effects of PWT2-[Dmt[1]] were assessed in different in vitro assays including receptor binding, stimulation of [^{35}S]GTPγS binding, calcium mobilization in cells co-expressing recombinant receptors and chimeric G proteins, and a BRET assay that measures receptor/G-protein and receptor/β-arrestin 2 interaction. Moreover, the putative analgesic action of PWT2-[Dmt[1]] has been investigated after i.t. administration in monkeys subjected to the tail withdrawal assay.

2. Materials and Methods

f 2.1 Synthesis of PWT2-[Dmt[1]]N/OFQ(1-13)

The PWT2 derivative of [Dmt[1]]N/OFQ(1-13) was prepared by using a convergent synthetic approach and methodology previously applied for the synthesis of PWT derivatives of N/OFQ (Guerrini et al., 2014), Neuropeptide S (Ruzza et al., 2015) and tachykinins (Ruzza et al., 2014). Firstly, [Dmt[1]Cys[14]]N/OFQ(1-14)-NH_2 was synthesised by solid phase method with an automatic solid phase peptide synthesizer Syro II (Biotage, Uppsala Sweden) using Fmoc/tBu chemistry (Benotoin NL., 2005). The resin 4-(2',4'-dimethoxyphenyl-Fmoc-aminomethyl)-phenoxyacetamido-norleucyl-MBHA (Rink amide MBHA resin) was used as a solid support. The resin was treated with 40% piperine/N,N-dimethylformamide (DMF)

and linked with Fmoc-Cys(Trt)-OH by using [O-(7-azabenzotriazol-1-yl)-1,1,3,3-tetramethyluronium hexafluorophosphate] (HATU) as the coupling reagent. The following Fmoc amino acids were sequentially coupled to the growing peptide chain: Fmoc-Lys(Boc)-OH, Fmoc-Arg(Pmc)-OH, Fmoc-Ala-OH, Fmoc-Ser(tBu)-OH, Fmoc-Lys(Boc)-OH, Fmoc-Arg(Pmc)-OH, Fmoc-Ala-OH, Fmoc-Gly-OH, Fmoc-Thr(^{t}Bu)-OH, Fmoc-Phe-OH, Fmoc-Gly-OH, Fmoc-Gly-OH, Fmoc-Dmt-OH (Dmt: 2',6'-dimethyl tyrosine). All the Fmoc amino acids (4 equiv) were coupled to the growing peptide chain by using HATU (4 equiv) in DMF in the presence of an equimolar concentration of 4-methylmorpholine (NMM), and the coupling reaction time was 1h. To improve the analytical profile of the crude peptide, capping with acetic anhydride (0.5M/DMF) in the presence of NMM (0.25M/DMF) (3:1 v/v; 2ml / 0.2 g of resin) was performed at any step. 40% Piperidine/DMF was used to remove the Fmoc. The protected peptide-resin was treated with reagent B (Sole', N.A. and Barany, G., 1992) (trifluoroacetic acid (TFA) / H_20 / phenol / triisopropylsilane 88 : 5 : 5: 2; v/v; 10 ml / 0.2 g of resin) for 1.5 h at room temperature. After filtration of the resin, the solvent was concentrated in vacuum and the residue triturated with ethyl ether. Crude [Dmt^{1}Cys^{14}]N/OFQ(1-14)-NH_2 was purified by preparative reversed-phase HPLC using a Water Delta Prep 3000 system with a Jupiter column C_{18} (250 × 30 mm, 300 A, 15 μm spherical particle size). The column was perfused at a flow rate of 20 ml/min with a mobile phase containing solvent A (5%, v/v, acetonitrile in 0.1% TFA), and a linear gradient from 5 to 40% of solvent B (60%, v/v, acetonitrile in 0.1% TFA) over 25 min for the elution of the peptide. Purified [Dmt^{1}Cys^{14}]N/OFQ(1-14)-NH_2 was reacted in solution with PWT2 core in a classical thio-Michael reaction using experimental conditions previously optimized for the synthesis of N/OFQ tetra branched derivatives (Rizzi et al., 2014). PWT2-[Dmt^1]N/OFQ(1-13) was purified using the same HPLC conditions employed for the purification of the linear [Dmt^{1}Cys^{14}]N/OFQ-NH_2.

Analytical HPLC analyses were performed on a Beckman 116 liquid chromatograph equipped with a Beckman 166 diode array detector. Analytical purity of [Dmt^{1}Cys^{14}]N/OFQ(1-14)-NH_2 and PWT2-[Dmt^1]N/OFQ(1-13) were determined using a Luna C_{18} column (4.6 × 100 mm, 3 μm particle size) with the above solvent system (solvents A and B) programmed at a flow rate of 0.5 ml / min using a linear gradient from 0% to 50% B over 25 min. Final product showed ≥ 95% purity when monitored at 220 nm. Molecular weight of PWT2-[Dmt^1]N/OFQ(1-13) (PWT2-Dmt^1]) was in accord with the expected molecular formula.

2.2 Membrane preparation

Cells were harvested, homogenized, and membrane fragments were resuspended in a wash buffer either consisting of 50 mM Tris-HCl pH to 7.4 with KOH, for CHO_{mu}, CHO_{delta}, and CHO_{kappa} or supplemented with 5 mM $MgSO_4$ for CHO_{NOP} cells in displacement binding assays, or in an homogenization buffer (50 mM Tris and 0.2 mM EGTA pH 7.4 with NaOH) in [^{35}S]GTPγS functional assays. The membrane suspensions were centrifuged and homogenized at 20,374 g at 4°C for 10 min repeating this process a total of 3 times. The resulting pellet was resuspended in an appropriate volume of the desired buffer and protein concentration measured using the Lowry assay (Lowry et al., 1951).

2.3 Receptor binding assay

Membrane protein (20~40 μg) was incubated in 0.5 ml of 50 mM Tris, 0.5% BSA and ~0.8 nM [^{3}H]-DPN for classical opioid or ~0.8 nM [^{3}H]-UFP-101 for NOP receptors, as well as varying concentrations (1 pM-10 μM) of the control ligands and test compounds. Non-specific binding was determined in the presence of 10 μM naloxone or 1 μM of N/OFQ for classical opioid and NOP receptors, respectively. Samples were incubated for 1 h at room temperature, following which reactions were terminated by vacuum filtration, onto PEI-soaked Whatman GF/B filters, using a Brandel harvester.

2.4 Stimulated [^{35}S]GTPγS binding assay

Membrane protein (20~40 μg) was incubated in 0.5 ml volume of 50 mM Tris, 0.2 mM EGTA, 1 mM $MgCl_2$, 100 mM NaCl, 0.1% BSA, 0.15 mM bacitracin; pH 7.4, GDP (33 μM), and ~150 pM [^{35}S]GTPγS. A range of concentrations of N/OFQ, [Dmt^1]N/OFQ(1-13)-NH_2 and PWT2-[Dmt^1] (1 pM - 10μM) was added prior to incubation. Non-specific binding was determined in the presence of unlabeled GTPγS (10 μM). Samples were incubated for 1 h at 30°C with gentle agitation. Reactions were terminated by vacuum filtration through dry Whatman GF/B filters, using a Brandel harvester.

2.5 Calcium mobilization assay

CHO cells stably coexpressing either human recombinant NOP, mu or kappa receptor along with the C-terminally modified $G\alpha_{qi5}$ chimeric protein and cells co-expressing the delta receptor and the $G\alpha_{qG66Di5}$ chimeric protein were generated as previously described (Camarda and Calo, 2013; Camarda et al., 2009). Cells were cultured in culture medium consisting of Dulbecco's modified Eagle's medium (DMEM)/HAMS F12 (1:1) supplemented with 10% fetal bovine serum (FBS), penicillin (100 IU/ml), streptomycin (100 μg/ml), L-glutamine (2 mM); fungizone (1 μg/ml), geneticin (G418; 200 μg/ml) and hygromycin B (100 μg/ml). Cell cultures were kept at 37 °C in 5% CO_2/humidified air. Cells were seeded at a density of 50,000 cells/well into 96-well black, clear-bottom plates. After 24 h incubation the cells were loaded with Hank's Balanced Salt Solution (HBSS) supplemented with 2.5 mM probenecid, 3 μM of the calcium sensitive fluorescent dye Fluo-4 AM, 0.01% pluronic acid and 20 mM HEPES (pH 7.4) for 30 min at 37 °C. Afterwards the loading solution was aspirated and a washing step with 100 μl/well of HBSS, HEPES (20 mM, pH 7.4), 2.5 mM probenecid and 500 μM Brilliant Black was carried out. Subsequently 100 μl/well of the same buffer was added. After placing cell culture and compound plates into the FlexStation II (Molecular Devices, Sunnyvale, CA, USA), fluorescence changes were measured after 10 min of stabilization at 37 °C. On-line additions were carried out in a volume of 50 μl/well.

2.6 BRET assay

Human Embryonic Kidney (HEK-293) and human SH-SY5Y neuroblastoma cells were grown in Dulbecco's modified Eagle's medium (DMEM) or Dulbecco's MEM/HAM'S F-12 (50/50) supplemented with 10% (v/v) FBS, penicillin G (100 IU/ml), streptomycin (100 μg/ml), L-glutamine (2 mM); fungizone (1 μg/ml), geneticin (G418; 200 μg/ml) and hygromycin B (100 μg/ml) either in a humidified atmosphere of 5% CO_2 at 37 °C. Cells

lines permanently co-expressing the different pairs of fusion proteins, NOP-RLuc/Gβ1-RGFP and NOP-RLuc/β-arrestin 2-RGFP (HEK293), mu-RLuc/Gβ1-RGFP and mu-RLuc/β-arrestin 2-RGFP (SH-SY5Y) were prepared using the pantropic retroviral expression system by Clontech as described previously (Molinari et al., 2010). For G-protein experiments enriched plasma membrane aliquots from transfected cells were prepared and quantified as previously described in detail (Malfacini et al., 2015). Luminescence in membranes was recorded in 96-well untreated white opaque microplates, while in whole cells in 96-well sterile poly-D-lysine-coated white opaque microplates for HEK-293 and in untreated white opaque microplates for SH-SY5Y cells using the luminometer Victor 2030 (PerkinElmer, Waltham, MA, USA). For the determination of receptor/G-protein interaction, membranes (3 μg of protein) prepared from cells co-expressing NOP/RLuc-Gβ1/RGFP or mu/RLuc-Gβ1/RGFP were added to wells in DPBS. For the determination of receptor/β-arrestin 2 interaction, cells co-expressing NOP/RLuc-β-arrestin 2/RGFP or mu/RLuc-β-arrestin 2/RGFP were plated 24 h before the experiment (100,000 cells $well^{-1}$). The cells were prepared for the experiment substituting the medium with PBS with $MgCl_2$ (0.5 mM) and $CaCl_2$ (0.9 mM). Coelenterazine at a final concentration of 5 μM was injected 15 min prior reading the cell plate. Different concentrations of ligands in 20 μl of PBS - BSA 0.01 % were added and incubated 15 min before reading luminescence. All the experiments were performed at room temperature.

2.7 Materials and drugs

All cell culture media and supplements were from Invitrogen (Paisley, U.K.). All other reagents used were from Sigma Chemical Co. (Poole, UK) or E. Merck (Darmstadt, Germany) and were of the highest purity available. Dermorphin, N/OFQ, [Dmt^1]N/OFQ(1-13)-NH_2 and PWT2-[Dmt^1] were synthesized in house (Department of Chemical and Pharmaceutical Sciences, University of Ferrara) as previously described (Guerrini et al., 1997; Guerrini et al., 2014), while J-113397, DPDPE, and dynorphin A were bought from Tocris Bioscience (Bristol, UK). Naltrexone HCl was from National Institute on Drug Abuse (Bethesda, MD, USA). Tritiated UFP-101 ([^{3}H]-UFP-101) was synthesized as described previously (Ibba et al., 2008). Tritiated diprenorphine ([^{3}H]-DPN) was purchased from Perkin Elmer. Native coelenterazine (CLZN, 5 mM, EtOH) was from Synchem UG & Co. KG (Altenburg, Germany). Stock solutions (1 mM) of peptides and the new compound PWT2-[Dmt^1] were made in ultrapure water and all stored at − 20°C until use. The successive dilutions were made in HBSS/HEPES (20 mM) buffer (containing 0.005 % Bovine Serum Albumin (BSA) fraction V to avoid licking) in the calcium assay and PBS/BSA (0.01 %) buffer in the BRET assay.

2.8 Animals

Four adult male and female rhesus monkeys (*Macaca mulatta,* aged 11-18 years old) weighing between 7.7 to 14 kg were used. Monkeys were individually housed and their daily diet consisted of approximately 25-30 biscuits (Purina Monkey Chow; Ralston Purina Co., St. Louis, MO, USA), fresh fruit, and water ad libitum. For 1 month before the present study, the monkeys were not exposed to any drugs. All monkeys had previously been trained in the warm water tail-withdrawal assay and they were housed in facilities accredited by the Association for Assessment and Accreditation of Laboratory Animal Care/AAALAC

International. All animal care and experimental procedures were conducted in accordance with the *Guide for the Care and Use of Laboratory Animals* as adopted and promulgated by the US National Institutes of Health (Bethesda, MD, USA) and approved by the Institutional Animal Care and Use Committee of Wake Forest University (Winston-Salem, NC, USA). All studies are reported in accordance with the ARRIVE guidelines for reporting experiments involving animals (Kilkenny et al., 2010).

2.9 In vivo studies

The warm water tail-withdrawal assay (Ko and Naughton, 2009) was used to evaluate thermal antinociceptive effect of PWT2-[Dmt^1]. Monkeys were seated in primate restraint chairs, and the lower parts of their shaved tails (approximately 15 cm) were immersed in a thermal flask containing water maintained at either 42, 46, or 50°C. Water at 42 and 46°C was used as non-noxious stimuli, and 50°C water was used as an acute noxious stimulus. Tail-withdrawal latencies were measured at each temperature by using a computerized timer by experimenters who were blinded to experimental conditions. If the monkeys did not remove their tails within 20 seconds (cut-off), the flask was removed and a maximum time of 20 seconds was recorded. Test sessions began with baseline measurements at each temperature. Subsequent tail-withdrawal latencies were measured at multiple time points after i.t administration of PWT2-[Dmt^1].

Behavioral activities of monkeys were recorded in their home cages for quantifying scratching responses, which is associated with itch sensation (Ko et al., 2004). Each 15-min recording session was conducted at multiple time points after i.t. administration of PWT2-[Dmt^1]. A scratch was defined as one brief (<1 second) episode of scraping contact of the forepaw or hind paw on the skin surface. Total scratches were counted for each 15-min session by experimenters who were blinded to experimental conditions.

PWT2-[Dmt^1] and naltrexone were dissolved in sterile water while J-113397 in a solution of dimethylsulfoxide/Tween 80/sterile water in a ratio of 1:1:8. PWT2-[Dmt^1] was administered i.t. in a volume of 1 ml through the subcutaneous access port in monkeys implanted with intrathecal catheters (Ding et al., 2015). Naltrexone and J-113397 were administered subcutaneously in a volume of 0.1 ml/kg. There was a minimum of 1-week interval between drug administrations.

We first characterized the effectiveness and duration of PWT2-[Dmt^1] against thermal nociception in monkeys. Monkeys received different doses (0.3-3 nmol) of i.t. PWT2-[Dmt^1] (0.3–3 nmol) or vehicle and their nociceptive thresholds were measured at multiple time points to determine the compound duration of action. In order to assess the involvement of a mu receptor component in PWT2-[Dmt^1]–mediated antinociception, we selected a fully effective antinociceptive dose (3 nmol) to determine if this dosing condition increased scratching behaviour (Ko et al., 2004). In addition, we selected a single dose 0.03 mg/kg of naltrexone and 0.1 mg/kg of J-113397, known to selectively produce mu and NOP receptor antagonist effects, respectively, in monkeys (Hu et al., 2010). Either antagonist was administered subcutaneously 1 h and 10 min after i.t. administration of 3 nmol of PWT2-[Dmt^1].

2.10 Data analysis and terminology

All data are expressed as means ± standard error of the mean (S.E.M.) of at least 3 experiments performed in duplicate. For potency values 95% confidence limits were indicated. The pharmacological terminology adopted in this report is consistent with the IUPHAR recommendations (Neubig et al., 2003). Receptor binding data are expressed as % displacement. [^{35}S]GTPγS data are expressed as stimulation factor that is the ratio between specific agonist stimulated [^{35}S]GTPγS binding and basal specific binding. Calcium mobilization data are expressed as fluorescence intensity units (FIU) in percent over the baseline. BRET data are calculated as BRET ratio between CPS measured for the RGFP and RLuc light emitted using 460(25) and 510(10) filters (PerkinElmer, Waltham, MA, USA), respectively. Data are expressed as stimulated BRET ratio obtained by subtracting the vehicle value from that measured in the presence of ligand. Affinity values are shown as pK_i calculated using the Cheng-Prusoff equation:

$$\mathrm{pK}_i = \log\left[\frac{IC_{50}}{1 + \frac{[L]}{K_D}}\right]$$

Where IC_{50} is the concentration of antagonist that produces 50% inhibition of the agonist response, [L] is the concentration of free radioligand and K_D is the dissociation constant of the radioligand for the receptor. Agonist potencies were given as pEC_{50} that is the negative logarithm to base 10 of the molar concentration of an agonist that produces 50% of the maximal possible effect. Maximal effects elicited by the agonists are expressed as intrinsic activity α using the control ligand as full agonist (α = 1.00). Concentration response curve to agonists were fitted with the four parameter logistic nonlinear regression model:

$$\mathrm{Effect}=\mathrm{baseline}+\frac{\mathrm{E_{max}} - \mathrm{baseline}}{1 + 10^{(\log \mathrm{EC_{50}} - \mathrm{X})\mathrm{n}}}$$

Where EC_{50} is the concentration of agonist producing a 50% maximal response, X is the agonist concentration and n is the Hill coefficient of the concentration response curve to the agonist. Curve fittings were performed using Graph Pad PRISM 5.0 (GraphPad Software In., San Diego, U.S.A.). Data obtained with calcium mobilization and BRET assays have been analysed statistically with one way ANOVA followed by the Dunnett's test for multiple comparisons, while data obtained with receptor binding assays (receptor binding and stimulated [^{35}S]GTPγS) with one way ANOVA followed by the Bonferroni's test for multiple comparisons. In both cases P values less than 0.05 were considered to be significant.

Antinociceptive effects were quantified in each animal as % maximum possible effect (MPE) at each time point and drug dose. The following formula was used to calculate %MPE: % MPE = [(Post-drug value for a behavioural response (s) – Pre-drug value for a behavioural response (s)/(Cutoff value 20 s – Pre-drug value for a behavioural response(s)) × 100]. If the animal did not withdraw its tail before the cut-off value, 100% MPE was assigned. Mean values (mean ± S.E.M.) were calculated from individual animals for all

behavioural end points. All in vivo data were analyzed by two-way analysis of variance with repeated measures followed by Bonferroni's multiple comparisons test. The criterion for significance for all tests was set at $P < 0.05$.

3. Results

3.1 Displacement Binding assay

In CHO_{NOP} cell membranes, N/OFQ and [Dmt^1]N/OFQ(1-13)-NH_2 displaced the binding of [^{3}H]-UFP-101 in a concentration dependent and saturable manner with high and similar values of affinity, i.e. 10.12 and 10.39 respectively. PWT2-[Dmt^1] displayed a significant decrease in affinity (pK_i 9.13) when compared to the parent compound [Dmt^1]N/OFQ(1-13)-NH_2 (Fig. 2A). Moreover, at high concentrations [Dmt^1]N/OFQ(1-13)-NH_2 displaced >100% of specific [^{3}H]-UFP-101 binding.

At mu sites dermorphin, [Dmt^1]N/OFQ(1-13)-NH_2 and its tetrameric derivative displaced the binding of [^{3}H]-DPN in a concentration dependent and saturable manner. [Dmt^1]N/OFQ(1-13)-NH_2 (pK_i 10.4) demonstrated higher affinity than dermorphin (9.14), while the affinity of the tetrameric compound was superimposable to that of dermorphin (9.25) (Fig. 2B). At CHO_{kappa} membranes, dynorphin A and [Dmt^1]N/OFQ(1-13)-NH_2 displaced the binding of [^{3}H]-DPN in a concentration dependent and saturable manner with high and similar (10.30 and 10.38) pK_i values. PWT2-[Dmt^1] showed an ~18 fold loss of affinity compared to its patent compound (Fig. 2C). Furthermore, all tested compounds displaced the binding of [^{3}H]-DPN at the delta receptor in a concentration dependent and saturable manner showing the following rank order of affinity: [Dmt^1]N/OFQ(1-13)-NH_2 > DPDPE > PWT2-[Dmt^1] (Fig. 2D). The values of affinity of [Dmt^1]N/OFQ(1-13)-NH_2 and its tetrabranced derivative are summarized in Table 1.

3.2 Stimulation of [^{35}S]GTPγS binding

N/OFQ and [Dmt^1]N/OFQ(1-13)-NH_2 stimulated the binding of [^{35}S]GTPγS in a concentration dependent and saturable manner in membranes prepared from CHO cells expressing the NOP receptor. [Dmt^1]N/OFQ(1-13)-NH_2 displayed slightly higher potency (9.46) and similar maximal effects (E_{max} as stimulation factor; 3.22 ± 0.22 fold) compared to those of N/OFQ (pEC_{50} 9.33, E_{max} 2.95 ± 0.10 fold). PWT2-[Dmt^1] mimicked the stimulatory effect of the parent compound with similar potency and maximal effects (Fig. 3A). In CHO_{mu} cell membranes, dermorphin and [Dmt^1]N/OFQ(1-13)-NH_2 stimulated the binding of [^{35}S]GTPγS in a concentration dependent and saturable manner. [Dmt^1]N/OFQ(1-13)-NH_2 showed a 3 fold increase in potency (8.58) and similar efficacy (3.06 ± 0.04 fold) compared to dermorphin (pEC_{50} 8.02, E_{max} 2.88 ± 0.05 fold). PWT2-[Dmt^1] behaved as the parent compound both in terms of potency (8.51) and maximal effects. (2.84 ± 0.11 fold) (Fig. 3B). In membranes from CHO_{kappa} cells, dynorphin A, [Dmt^1]N/OFQ(1-13)-NH_2 and the PWT compound stimulated the binding of [^{35}S]GTPγS in a concentration dependent and saturable manner with similar potency (9.19, 9.14, 9.20 respectively). [Dmt^1]N/OFQ(1-13)-NH_2 and its PWT derivative produced significantly higher maximal responses (2.51 ± 0.17 fold, 2.43 ± 0.08 fold) compared to that elicited by the endogenous compound dynorphin A (2.03 ± 0.04 fold) (Fig. 3C). In parallel experiments performed in

membranes expressing the delta receptor, the standard compound DPDPE, [Dmt^1]N/OFQ(1-13)-NH_2 and its PWT derivative stimulated the binding of [^{35}S]GTPγS in a concentration dependent manner with similar potency and efficacy (Fig. 3D). Potency and efficacy values for [Dmt^1]N/OFQ(1-13)-NH_2 and its PWT derivative are summarized in Table 2.

3.3 Calcium mobilization assay

In CHO cells coexpressing NOP and $G\alpha_{qi5}$, N/OFQ increased intracellular calcium levels in a concentration dependent manner with high potency (9.59) and maximal effects of 316 ± 51% over the basal value. In parallel experiments [Dmt^1]N/OFQ(1-13)-NH_2 and PWT2-[Dmt^1] mimicked the effect of the N/OFQ with similar maximal effects but with reduced potency of 3 and 58 fold, respectively (Fig. 4A). In CHO cells stably expressing the chimeric protein $G\alpha_{qi5}$ and the human mu receptor, dermorphin produced a concentration dependent stimulation of calcium mobilization with high potency (8.19) and maximal effects (345 ± 14% over basal). [Dmt^1]N/OFQ(1-13)-NH_2 and PWT2-[Dmt^1] elicited similar stimulatory actions, however with slightly lower maximal effects (306 ± 10% and 283 ± 3%) and potencies 3 and 23 fold, respectively (Fig. 4B). In CHO_{kappa} cells stably expressing the $G\alpha_{qi5}$ chimeric protein the reference agonist dynorphin A evoked a concentration dependent increase in calcium mobilization with high potency (8.54) and maximal effects of 206 ± 31 % over the basal values (Fig. 4C). In parallel experiments [Dmt^1]N/OFQ(1-13)-NH_2 stimulated calcium release with 8 fold lower potency (7.66) and maximal effects (191 ± 26 %) not far from those of dynorphin A. PWT2-[Dmt^1] mimicked the stimulatory effect of the parent compound with similar maximal effects; however there was a substantial loss of potency (Fig. 4C). Finally in CHO_{delta} cells stably expressing the $G\alpha_{qG66Di5}$ chimeric protein the reference agonist DPDPE evoked a concentration dependent increase in calcium levels with a potency of 8.15 and maximal effect of 238 ± 27% over the basal values. Compounds [Dmt^1]N/OFQ(1-13)-NH_2 and PWT2-[Dmt^1] elicited slightly lower maximal effects with potency 8 and 23 fold lower than DPDPE (Fig. 4D). The values of potency and efficacy of [Dmt^1]N/OFQ(1-13)-NH_2 and its PWT derivative are summarized in Table 3.

3.4 BRET assay

The ability to promote receptor/G protein and receptor/β-arrestin 2 interaction of standard ligands, (i.e. N/OFQ for the NOP receptor and dermorphin for the mu receptor), [Dmt^1]N/OFQ(1-13)-NH_2 and its PWT derivative, has been assessed using a BRET based assay. As shown in Fig. 5A, in membranes prepared from cells HEK-293 expressing the NOP receptor, N/OFQ, [Dmt^1]N/OFQ(1-13)-NH_2 and its PWT derivative promoted receptor/G protein interaction in a concentration dependent manner with similar potency and maximal effects. Under the same experimental conditions, membranes extracted from SH-SY5Y cells were used to evaluate the activity of the compounds at the mu receptor. Dermorphin promoted mu/G-protein interaction in a concentration dependent manner with high potency. [Dmt^1]N/OFQ(1-13)-NH_2 mimicked the stimulatory effect of the standard with a similar maximal response but 6 fold higher potency. PWT2-[Dmt^1] promoted mu/G-protein interaction with a potency close to that of the parent compound. Interestingly PWT2-[Dmt^1] at micromolar concentrations elicited stimulatory effect higher than those of the standard (Fig. 5B). These results are summarized in table 4.

In HEK-293 cells expressing the NOP receptor N/OFQ promoted receptor/β-arrestin 2 interaction in a concentration dependent manner with high potency. [Dmt^1]N/OFQ(1-13)-NH_2 mimicked the stimulatory effect of the standard with similar potency but with a lower maximal response. PWT2-[Dmt^1] showed a lower potency and efficacy compared to the standard and parent compound, behaving as partial agonist (Fig. 6A). In SH-SY5Y cells expressing the mu receptor dermorphin promoted receptor/β-arrestin 2 interaction in a concentration dependent manner with high potency. [Dmt^1]N/OFQ(1-13)-NH_2 demonstrated a similar potency associated with a reduction in maximal effects. PWT2-[Dmt^1] acted in a similar manner to the parent compound but with slightly lower potency (Fig. 6B).

In Fig. 7, the concentration response curves to standard agonists, [Dmt^1]N/OFQ(1-13)-NH_2, and PWT2-[Dmt^1] at G protein and arrestin are plotted in the same graph. It can be seen that the PWT modification favoured G protein vs arrestin potency and efficacy; this applies to both NOP and mu receptors. This is made clearer in Fig. **8** where the bias plot obtained by plotting the amount of signal produced in the G protein pathway as a function of equal amounts of signal produced in the arrestin pathway in response to equimolar concentrations of agonist (Kenakin, 2014).

3.5 In vivo studies

I.t. administration of PWT2-[Dmt^1] in monkeys produced antinociception against an acute nociceptive stimulus (50°C water) in both a dose-[$F(3,9) = 241.9$; $P < 0.05$] and time-dependent [$F(6,18) = 139.5$; $P < 0.05$] manner. Multiple comparison testing indicated that 0.3 nmol of intrathecal PWT2-[Dmt^1] produced antinociception for 2 h, while the antinociceptive effects produced by 1 and 3 nmol PWT2-[Dmt^1] last for 6 and 24 h, respectively (Fig. 9A). The higher dose (3 nmol) of PWT2-[Dmt^1] did not significantly elicit scratching responses at any time point [$F(3, 6) = 1.7$; $P = 0.27$] (Fig. 9B). I.t. PWT2-[Dmt^1] at doses 0.3-3 nmol did not cause any overt side effects including sedation or motor impairment.

Fig. 10 shows the effects of antagonists on intrathecal PWT2-[Dmt^1] (3 nmol)-induced antinociception in monkeys. There were significant differences among these antagonist dosing conditions [$F(2,6) = 226.5$; $P < 0.05$]. Multiple comparison testing indicated that the NOP receptor antagonist J-113397 (0.1 mg/kg) significantly blocked i.t. PWT2-[Dmt^1]-induced antinociception while naltrexone 0.03 mg/kg was inactive.

4. Discussion

Previous studies demonstrated that [Dmt^1]N/OFQ(1-13)-NH_2 behaves as a potent agonist for NOP and classical opioid receptors and elicits robust antinociceptive effects after spinal administration in non-human primates (Molinari et al., 2013). The recently developed PWT strategy (Guerrini et al., 2014) has been applied to [Dmt^1]N/OFQ(1-13)-NH_2 generating the tetrabranched derivative PWT2-[Dmt^1]. In receptor binding studies, PWT2-[Dmt^1] displayed approximately 10 fold lower affinity than the parent peptide, but maintained a similar profile of selectivity. In functional studies performed with different assays, PWT2-[Dmt^1] always behaved, similar to [Dmt^1]N/OFQ(1-13)-NH_2, as a full agonist. Moreover PWT2-[Dmt^1] potency was in general similar to that of the parent peptide. After i.t.

administration in monkeys PWT2-[Dmt^1] elicited antinociceptive effects and was at least 10 fold more potent than [Dmt^1]N/OFQ(1-13)-NH_2 and produced longer lasting effects. Collectively this study corroborated previous findings (Rizzi et al., 2014; Rizzi et al., 2015; Ruzza et al., 2014; Ruzza et al., 2015) demonstrating that the PWT approach can be applied to the peptide sequence of different GPCR peptide agonists to generate novel ligands characterized by a similar in vitro pharmacological profile associated with high potency and long lasting action in vivo.

In receptor binding studies performed on membranes from cells expressing recombinant human receptors standard ligands for NOP and opioid receptors i.e. N/OFQ, dermorphin, dynorphin A and DPDPE displayed high affinity for their respective receptors with pK_i values in line with previous findings (Molinari et al., 2013; Reisine, 1995). [Dmt^1]N/OFQ(1-13)-NH_2 was able to displace radioligand binding at the four receptors with the following rank order of affinity NOP = mu = kappa > delta. These results perfectly match previous studies both in terms of absolute values and rank order of affinity corroborating the proposal of [Dmt^1]N/OFQ(1-13)-NH_2 as a universal opioid receptor ligand (Molinari et al., 2013). PWT2-[Dmt^1] was also able to bind to NOP and classical opioid receptors. Interestingly in NOP membranes PWT2-[Dmt^1] displaced an amount of radioactivity higher than N/OFQ. We interpret these perplexing results as due to the presence of displaceable nonspecific binding, a phenomenon relatively common when N/OFQ or N/OFQ related peptides are used as radioligands (Dooley and Houghten, 2000). Compared to [Dmt^1]N/OFQ(1-13)-NH_2, PWT2-[Dmt^1] displayed approximately 10 fold lower affinity at all receptors; as a consequence the profile of selectivity of PWT2-[Dmt^1] is identical to that of the parent peptide. These results are similar to those previously obtained with PTW2-N/OFQ that maintained high NOP selectivity typical of the natural peptide (Rizzi et al., 2014). However it must be noted that PTW2-N/OFQ displayed slightly higher affinity than N/OFQ while the opposite is true for [Dmt^1]N/OFQ(1-13)-NH_2 and PWT2-[Dmt^1].

In [^{35}S]GTPγS binding experiments, standard agonists displayed high potency and efficacy for their receptors. Data obtained at NOP and mu receptor are superimposable to our previous findings (delta and kappa were not assessed in Molinari et al. (2013)). [Dmt^1]N/OFQ(1-13)-NH_2 behaved as full agonist with the following rank order of receptor potency NOP > kappa > mu > delta. This is similar to that obtained in receptor binding experiments and, limited to NOP and mu, in previous [^{35}S]GTPγS experiments (Molinari et al., 2013). In parallel experiments PWT2-[Dmt^1] mimicked the effects of [Dmt^1]N/OFQ(1-13)-NH_2 displaying similar potency and maximal effects at all four receptors. Thus these results demonstrated that application of PWT to the [Dmt^1]N/OFQ(1-13)-NH_2 sequence does not modify its pharmacological activity i.e. full agonism. This finding is in line with a large series of previous studies in which the pharmacological activity of different peptide sequences including the full agonists N/OFQ (Rizzi et al., 2014), substance P, neurokinin A and B (Ruzza et al., 2014), neuropeptide S (Ruzza et al., 2015), and dermorphin (Ferrari et al., unpublished) was maintained by PWT derivatives.

The calcium mobilization assay used to characterize the pharmacological profile of PWT2-[Dmt^1] has been previously validated with a large panel of NOP and opioid ligands (Camarda and Calo, 2013; Camarda et al., 2009) and the standard agonists used in the

present investigation displayed potencies and selectivity profiles in line with the above mentioned studies. [Dmt^1]N/OFQ(1-13)-NH_2 mimicked the stimulatory effects of standards at the four receptors displaying similar maximal effects and the following rank order of receptor potency NOP > mu = kappa > delta. Superimposable results were previously obtained both in terms of absolute potencies and selectivity profile (Molinari et al., 2013). PWT2-[Dmt^1] was also able to stimulate in a concentration dependent manner calcium mobilization in the four cell lines. Compared to [Dmt^1]N/OFQ(1-13)-NH_2 the tetrabranched derivative showed similar maximal effects and selectivity profile but with reduced potency by 3 to 30 fold. This result is in line with receptor binding findings but contrasts with those obtained in the [^{35}S]GTPγS binding assay. It is worthy of mention that similar findings i.e. reduced potency of PWT derivatives in the calcium assay compared to other functional assays have been previously obtained with N/OFQ (Rizzi et al., 2014), substance P, neurokinin A and B (Ruzza et al., 2014), and dermorphin (Ferrari et al., unpublished) but not with neuropeptide S (Ruzza et al., 2015). The loss in agonist potency of PWT derivatives in the calcium mobilization assay has been interpreted as a due to non-equilibrium conditions (Charlton and Vauquelin, 2010). In fact PWT derivatives display slow kinetics of action as revealed in isolated tissue experiments (Rizzi et al., 2014; Ruzza et al., 2014). The relatively long time needed to obtain full receptor activation by slowly equilibrating agonists is not compatible with the rapid and transient nature of the calcium response (Charlton and Vauquelin, 2010).

The BRET assay used to investigate the ability of [Dmt^1]N/OFQ(1-13)-NH_2 and PWT2-[Dmt^1] to promote receptor interaction with G protein and β-arrestin 2 has been previously validated for classical opioid (Molinari et al., 2010) as well as NOP receptors (Malfacini et al., 2015) and then used for characterizing novel ligands (Asth et al., 2016; Bird et al., 2016; Rizzi et al., 2016) or for selecting the best compounds for inducing receptor stability and crystallogenesis (Miller et al., 2015). In line with previous findings (Malfacini et al., 2015; Rizzi et al., 2016), the standard peptides N/OFQ and dermorphin behaved as potent and selective agonists in promoting receptor interaction both with G protein and β-arrestin 2. [Dmt^1]N/OFQ(1-13)-NH_2 was able to similarly promote receptor interaction with G protein and β-arrestin at NOP and mu receptors. The effects of the peptide were similar to those of the standards both in term of potency and maximal effects. The results obtained with the standards and [Dmt^1]N/OFQ(1-13)-NH_2 with the BRET receptor/G protein assay and with the [^{35}S]GTPγS binding assay are virtually superimposable. This confirms our previous findings obtained with a large panel of NOP (Malfacini et al., 2015) and opioid (Molinari et al., 2010) receptor ligands. As far as PWT2-[Dmt^1] is concerned, in BRET/G protein experiments this compound displayed similar potency and efficacy as [Dmt^1]N/OFQ(1-13)-NH_2 at both NOP and mu receptors while in BRET/ β-arrestin studies it displayed reduced potency (particularly at mu) associated with reduced efficacy (particularly at NOP). Thus, as directly shown by the bias plot, PWT2-[Dmt^1] behaved as a G protein biased agonist both at NOP and mu receptors. Similar results have been previously obtained by applying the PWT technology to N/OFQ. In fact an inversion in the rank order of potency between N/OFQ and PWT2-N/OFQ was measured in NOP/G protein and NOP/β-arrestin studies. PWT2-N/OFQ was more potent than the natural agonist in promoting G protein interaction, but less potent than N/OFQ in inducing arrestin interaction (Malfacini et al., 2015). Thus similar to PWT2-

[Dmt^1], PWT2-N/OFQ also behaved as G protein biased agonist. The interpretation of these findings is far from being obvious. In fact the N terminal pharmacophoric peptide sequences i.e. Phe-Gly-Gly-Phe and Dmt-Gly-Gly-Phe of N/OFQ and [Dmt^1]N/OFQ(1-13)-NH_2, respectively, are identical in the PWT derivatives of the two peptides and recent receptor structure (Thompson et al., 2012; Miller et al., 2015) and modelling (Daga and Zaveri, 2012; Kothandan et al., 2014) studies demonstrated that receptor activation is triggered by the occupation of the NOP receptor binding pocked by these sequences. Eventually when linked together into the PWT structure the N terminal pharmacophoric sequences lose the ability to adopt some conformational states that are more important for promoting the interaction of the receptor with β-arrestin than with G protein. However these are mere speculations that should be validated experimentally by solving the structure of the NOP receptor in complex with peptides, their PWT derivatives, G protein and β-arrestin. Moreover the ability to promote G protein biased agonism by applying the PWT chemical modification is not a general phenomenon. This has been demonstrated for the PWT derivatives of N/OFQ and [Dmt^1]N/OFQ(1-13)-NH_2 but not for PWT2-dermorphin. In fact, the latter peptide maintained the unbiased behaviour of the natural peptide in BRET experiments (Ferrari et al., unpublished).

Previous studies demonstrated that after spinal administration in monkeys [Dmt^1]N/OFQ(1–13)-NH_2 elicits a robust and dose dependent (1 – 10 nmol) antinociceptive effect (Molinari et al., 2013). PWT2-[Dmt^1] mimicked the antinociceptive action of the parent peptide being approximately 10 fold more potent. The lack of a direct comparison in the same series of experiments of the time course of the action of [Dmt^1]N/OFQ(1–13)-NH_2 and PWT2-[Dmt^1] does not allow a detailed discussion regarding the duration of action. However the duration of action of the ED_{50} dose of [Dmt^1]N/OFQ(1–13)-$NH_2$is less than 90 min (Molinari et al., 2013) while that of PWT2-[Dmt^1] is between 2 and 6 h. Importantly the dose of 3 nmol of PWT2-[Dmt^1] was able to elicit statistically significant effects even 24 h after injection. These results confirm and extend previous findings (Rizzi et al., 2014; Rizzi et al., 2015; Ruzza et al., 2014; Ruzza et al., 2015) demonstrating that the PWT strategy generates tetrabranched derivatives characterized by a pharmacological profile similar to the native peptide in vitro, but associated with a higher potency and a marked prolongation of action in vivo. Antagonist experiments were performed in order to investigate the receptor(s) involved in the antinociceptive action of PWT2-[Dmt^1]. J-113397 but not naltrexone was able to fully reverse the action of PWT2-[Dmt^1]. Similar results were previously obtained with NOP selective agonists such as N/OFQ (Ko et al., 2006) and UFP-112 (Hu et al., 2010). Thus these findings suggest that the spinal antinociceptive action of PWT2-[Dmt^1] at doses of 0.3-3 nmol is exclusively due to NOP receptor activation. This contrasts with the low level of NOP selectivity (range 2 – 10 fold) displayed by PWT2-[Dmt^1] in in vitro functional assays. Species specific differences may account for this discrepancy although available evidence suggests no major pharmacological differences between human and monkey NOP receptors (Koga et al., 2009). Further studies are needed in order to modify the [Dmt^1]N/OFQ(1–13)-NH_2 sequence with the aim of generating a mixed NOP/opioid ligand with exactly the same potency at NOP and mu receptors. The PWT derivative of such ligand may promote robust and long lasting analgesic effects based on the well described synergistic action of NOP and mu receptor activation (reviewed in Toll et al. (2016)). The promising

results obtained with the mixed agonist cebranopadol (Schunk et al., 2014) in preclinical (Linz et al., 2014; Rizzi et al., 2016) as well as clinical studies (Lambert et al., 2015) corroborate this proposal.

In conclusion this study demonstrated that the application of the PWT technology to the peptide sequence of [Dmt^1]N/OFQ(1-13)-NH_2 generated a tetrabranched derivative that maintains in vitro the universal opioid agonist features of the parent peptide associated with a certain degree of G protein biased agonism. Confirming previous findings obtained with different peptide sequences, the in vivo action of PWT2-[Dmt^1] was characterized by high potency associated with long lasting action. Despite its limited NOP over opioid receptor selectivity in vitro, receptor antagonist studies demonstrated that the spinal analgesic effects PWT2-[Dmt^1] in non human primates, at least in the examined range of doses, was exclusively due to NOP receptor activation.

References

Asth L, Ruzza C, Malfacini D, Medeiros I, Guerrini R, Zaveri NT, Gavioli EC, Calo G. Beta-arrestin 2 rather than G protein efficacy determines the anxiolytic-versus antidepressant-like effects of nociceptin/orphanin FQ receptor ligands. Neuropharmacology. 2016; 105:434–442. [PubMed: 26867504]

Benoiton, NL. Chemistry of Peptide Synthesis. Taylor & Francis; London: 2005. p. 125-154.

Bird MF, Cerlesi MC, Brown M, Malfacini D, Vezzi V, Molinari P, Micheli L, Di Cesare Mannelli L, Ghelardini C, Guerrini R, Calo' G, Lambert DG. Characterisation of the novel mixed Mu-NOP peptide ligand dermorphin-N/OFQ (DeNo). PloS one. 2016 in press.

Camarda V, Calo G. Chimeric g proteins in fluorimetric calcium assays: experience with opioid receptors. Methods Mol Biol. 2013; 937:293–306. [PubMed: 23007594]

Camarda V, Fischetti C, Anzellotti N, Molinari P, Ambrosio C, Kostenis E, Regoli D, Trapella C, Guerrini R, Severo S, Calo G. Pharmacological profile of NOP receptors coupled with calcium signaling via the chimeric protein G alpha qi5. Naunyn Schmiedebergs Arch Pharmacol. 2009; 379:599–607. [PubMed: 19183962]

Charlton SJ, Vauquelin G. Elusive equilibrium: the challenge of interpreting receptor pharmacology using calcium assays. Br J Pharmacol. 2010; 161:1250–1265. [PubMed: 20977466]

Daga PR, Zaveri NT. Homology modeling and molecular dynamics simulations of the active state of the nociceptin receptor reveal new insights into agonist binding and activation. Proteins. 2012; 80:1948–1961. [PubMed: 22489047]

Ding H, Hayashida K, Suto T, Sukhtankar DD, Kimura M, Mendenhall V, Ko MC. Supraspinal actions of nociceptin/orphanin FQ, morphine and substance P in regulating pain and itch in non-human primates. Br J Pharmacol. 2015; 172:3302–3312. [PubMed: 25752320]

Dooley CT, Houghten RA. Orphanin FQ/nociceptin receptor binding studies. Peptides. 2000; 21:949–960. [PubMed: 10998528]

Guerrini R, Calo G, Rizzi A, Bianchi C, Lazarus LH, Salvadori S, Temussi PA, Regoli D. Address and message sequences for the nociceptin receptor: a structure-activity study of nociceptin-(1-13)-peptide amide. J Med Chem. 1997; 40:1789–1793. [PubMed: 9191955]

Guerrini R, Marzola E, Trapella C, Pela M, Molinari S, Cerlesi MC, Malfacini D, Rizzi A, Salvadori S, Calo G. A novel and facile synthesis of tetra branched derivatives of nociceptin/orphanin FQ. Bioorg Med Chem. 2014; 22:3703–3712. [PubMed: 24878361]

Hu E, Calo G, Guerrini R, Ko M. Long lasting antinociceptive spinal effects in primates of the novel nociceptin/orphanin FQ receptor agonist UFP-112. Pain. 2010; 148:107–113. [PubMed: 19945794]

Ibba M, Kitayama M, McDonald J, Calo G, Guerrini R, Farkas J, Toth G, Lambert DG. Binding of the novel radioligand [(3)H]UFP-101 to recombinant human and native rat nociceptin/orphanin FQ receptors. Naunyn Schmiedebergs Arch Pharmacol. 2008; 378:553–561. [PubMed: 18807245]

Kenakin, T. A Pharmacology Primer. Fourth. Elsevier Academic Press; China: 2014.

Kilkenny C, Browne W, Cuthill IC, Emerson M, Altman DG. Animal research: reporting in vivo experiments: the ARRIVE guidelines. Br J Pharmacol. 2010; 160:1577–1579. [PubMed: 20649561]

Ko MC, Naughton NN. Antinociceptive effects of nociceptin/orphanin FQ administered intrathecally in monkeys. J Pain. 2009; 10:509–516. [PubMed: 19231294]

Ko MC, Song MS, Edwards T, Lee H, Naughton NN. The role of central mu opioid receptors in opioid-induced itch in primates. J Pharmacol Exp Ther. 2004; 310:169–176. [PubMed: 15044556]

Ko MC, Wei H, Woods JH, Kennedy RT. Effects of Intrathecally Administered Nociceptin/Orphanin FQ in Monkeys: Behavioral and Mass Spectrometric Studies. J Pharmacol Exp Ther. 2006; 318:1257–1264. [PubMed: 16766718]

Koga K, Ichikawa D, Nambu H, Azuma-Kanoh T, Sakai N, Takaki-Kawagoe H, Ozaki S, Ohta H. Cloning and characterization of the rhesus monkey nociceptin/orphanin FQ receptor. Genes & genetic systems. 2009; 84:319–325. [PubMed: 20154418]

Kothandan G, Gadhe CG, Balupuri A, Ganapathy J, Cho SJ. The nociceptin receptor (NOPR) and its interaction with clinically important agonist molecules: a membrane molecular dynamics simulation study. Molecular bioSystems. 2014; 10:3188–3198. [PubMed: 25259728]

Lambert DG, Bird MF, Rowbotham DJ. Cebranopadol: a first in-class example of a nociceptin/orphanin FQ receptor and opioid receptor agonist. British journal of anaesthesia. 2015; 114:364–366. [PubMed: 25248647]

Linz K, Christoph T, Tzschentke TM, Koch T, Schiene K, Gautrois M, Schroder W, Kogel BY, Beier H, Englberger W, Schunk S, De Vry J, Jahnel U, Frosch S. Cebranopadol: a novel potent analgesic nociceptin/orphanin FQ peptide and opioid receptor agonist. J Pharmacol Exp Ther. 2014; 349:535–548. [PubMed: 24713140]

Lowry OH, Rosenbrough NJ, Farr AL, Randall RJ. Protein measurement with the Folin phenol reagent. J Biol Chem. 1951; 193:265–275. [PubMed: 14907713]

Malfacini D, Ambrosio C, Gro MC, Sbraccia M, Trapella C, Guerrini R, Bonora M, Pinton P, Costa T, Calo G. Pharmacological Profile of Nociceptin/Orphanin FQ Receptors Interacting with G-Proteins and beta-Arrestins 2. PloS one. 2015; 10:e0132865. [PubMed: 26248189]

Miller RL, Thompson AA, Trapella C, Guerrini R, Malfacini D, Patel N, Han GW, Cherezov V, Calo G, Katritch V, Stevens RC. The Importance of Ligand-Receptor Conformational Pairs in Stabilization: Spotlight on the N/OFQ G Protein-Coupled Receptor. Structure. 2015; 23:2291–2299. [PubMed: 26526853]

Molinari P, Vezzi V, Sbraccia M, Gro C, Riitano D, Ambrosio C, Casella I, Costa T. Morphine-like opiates selectively antagonize receptor-arrestin interactions. J Biol Chem. 2010; 285:12522–12535. [PubMed: 20189994]

Molinari S, Camarda V, Rizzi A, Marzola G, Salvadori S, Marzola E, Molinari P, McDonald J, Ko MC, Lambert DG, Calo G, Guerrini R. [Dmt1]N/OFQ(1-13)-NH2: a potent nociceptin/orphanin FQ and opioid receptor universal agonist. Br J Pharmacol. 2013; 168:151–162. [PubMed: 22827708]

Neubig RR, Spedding M, Kenakin T, Christopoulos A. International Union of Pharmacology Committee on Receptor Nomenclature and Drug Classification. XXXVIII. Update on terms and symbols in quantitative pharmacology. Pharmacol Rev. 2003; 55:597–606. [PubMed: 14657418]

Reisine T. Opiate receptors. Neuropharmacology. 1995; 34:463–472. [PubMed: 7566479]

Rizzi A, Cerlesi MC, Ruzza C, Malfacini D, Ferrari F, Bianco S, Costa T, Guerrini R, Trapella C, Calo' G. Pharmacological characterization of cebranopadol a novel analgesic acting as mixed nociceptin/orphanin FQ and opioid receptor agonist. Pharma Res Per. 2016; 4:e00247.

Rizzi A, Malfacini D, Cerlesi MC, Ruzza C, Marzola E, Bird MF, Rowbotham DJ, Salvadori S, Guerrini R, Lambert DG, Calo G. In vitro and in vivo pharmacological characterization of nociceptin/orphanin FQ tetrabranched derivatives. Br J Pharmacol. 2014; 171:4138–4153. [PubMed: 24903280]

Rizzi A, Sukhtankar DD, Ding H, Hayashida K, Ruzza C, Guerrini R, Calo G, Ko MC. Spinal antinociceptive effects of the novel NOP receptor agonist PWT2-nociceptin/orphanin FQ in mice and monkeys. Br J Pharmacol. 2015; 172:3661–3670. [PubMed: 25828800]

Ruzza C, Rizzi A, Malfacini D, Cerlesi MC, Ferrari F, Marzola E, Ambrosio C, Gro C, Severo S, Costa T, Calo G, Guerrini R. Pharmacological characterization of tachykinin tetrabranched derivatives. Br J Pharmacol. 2014; 171:4125–4137. [PubMed: 24758475]

Ruzza C, Rizzi A, Malfacini D, Pulga A, Pacifico S, Salvadori S, Trapella C, Reinscheid RK, Calo G, Guerrini R. In vitro and in vivo pharmacological characterization of a neuropeptide S tetrabranched derivative. Pharmacology research & perspectives. 2015; 3:e00108. [PubMed: 25692025]

Schunk S, Linz K, Hinze C, Frormann S, Oberborsch S, Sundermann B, Zemolka S, Englberger W, Germann T, Christoph T, Kogel BY, Schroder W, Harlfinger S, Saunders D, Kless A, Schick H, Sonnenschein H. Discovery of a Potent Analgesic NOP and Opioid Receptor Agonist: Cebranopadol. ACS medicinal chemistry letters. 2014; 5:857–862. [PubMed: 25147603]

Sole' NA, Barany G. Optimization of solid-phase synthesis of [Ala8]-dynorphin. Journal Organic Chemistry. 1992; 57:5399–5403.

Thompson AA, Liu W, Chun E, Katritch V, Wu H, Vardy E, Huang XP, Trapella C, Guerrini R, Calo G, Roth BL, Cherezov V, Stevens RC. Structure of the nociceptin/orphanin FQ receptor in complex with a peptide mimetic. Nature. 2012; 485:395–399. [PubMed: 22596163]

Toll L, Bruchas MR, Calo G, Cox BM, Zaveri NT. Nociceptin/Orphanin FQ Receptor Structure, Signaling, Ligands, Functions, and Interactions with Opioid Systems. Pharmacol Rev. 2016; 68:419–457. [PubMed: 26956246]

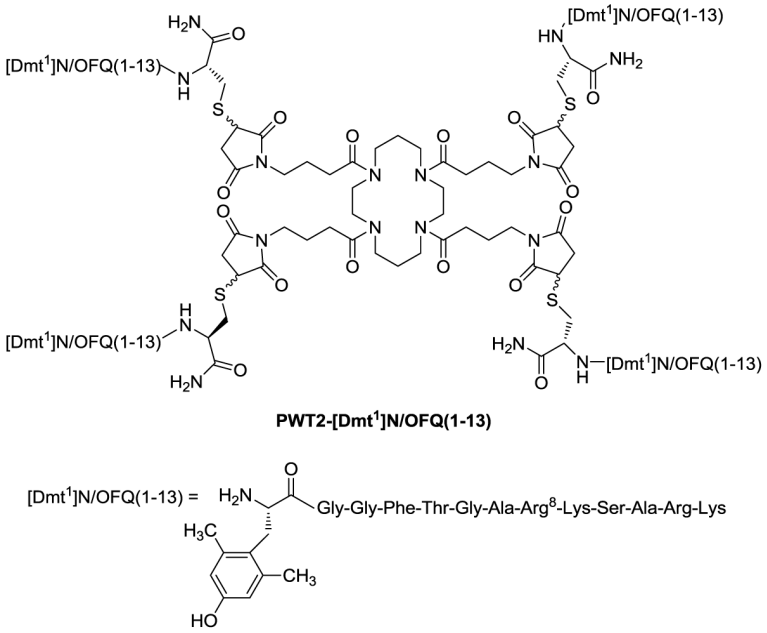

Figure 1.
Chemical structure of the compound PWT2-[Dmt[1]].

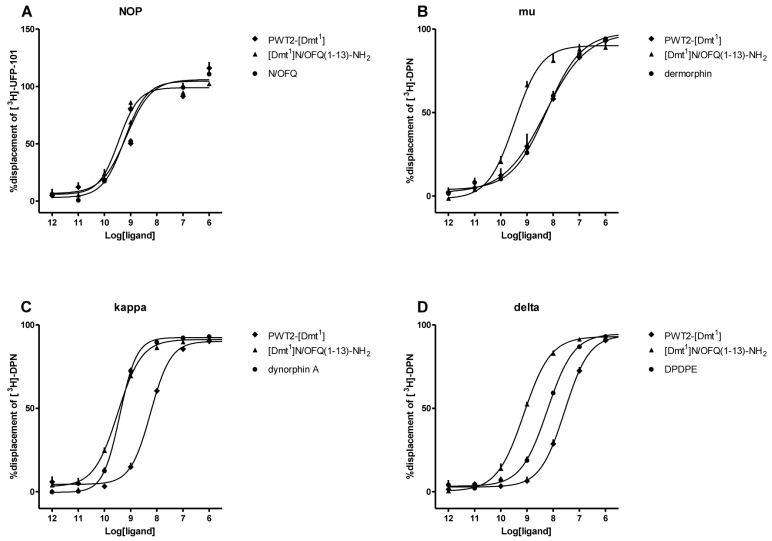

Figure 2.

Displacement binding studies. Displacement of [^{3}H]UFP-101 at CHO_{NOP} cell membranes and of [^{3}H]DPN at $CHO_{mu/kappa/delta}$ cell membranes by respective control ligand, [Dmt^1]N/OFQ(1-13)-NH_2 and PWT2-[Dmt^1]. Data are the mean ± S.E.M. of at least 5 separate experiments performed in duplicate.

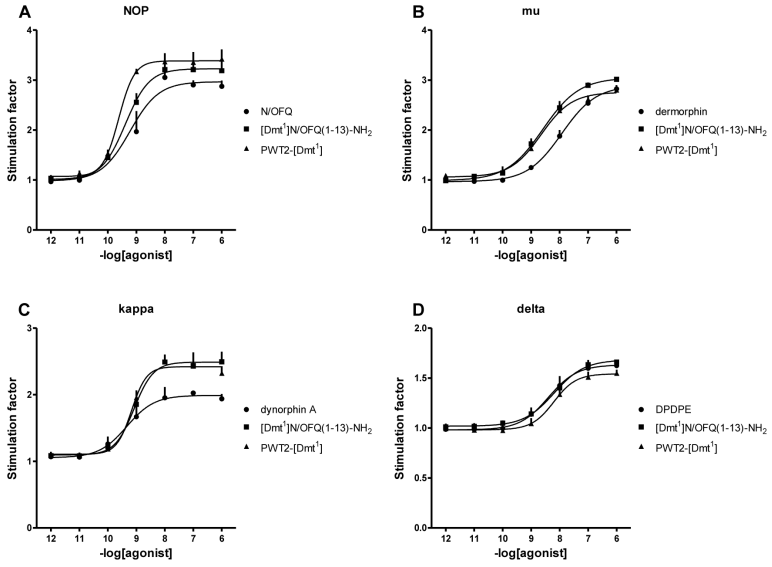

Figure 3.

[^{35}S]GTPγS binding studies. Concentration response curves to standard agonists, [Dmt^{1}]N/OFQ(1-13)-NH_2 and PWT2-[Dmt^{1}] in membranes of CHO cells stably expressing NOP or classical opioid receptors. Data are the mean ± S.E.M. for n≥5 separate experiments.

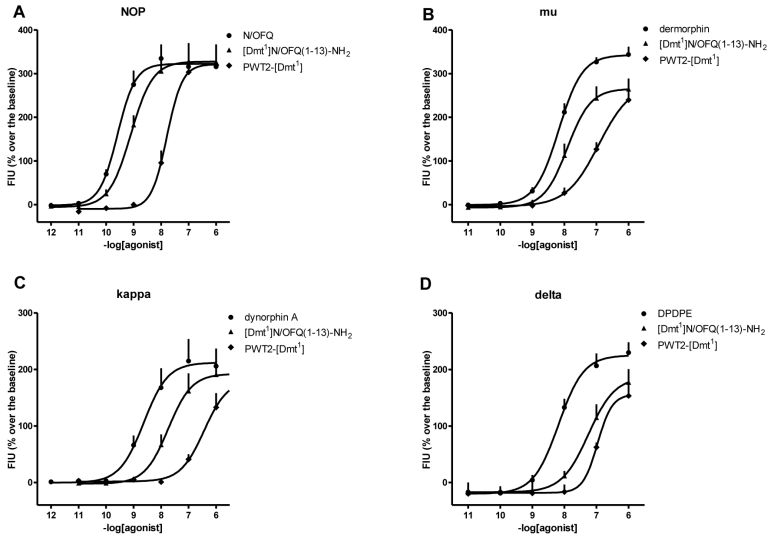

Figure 4.

Calcium mobilization studies. Concentration response curves to standard agonists, [Dmt^1]N/OFQ(1-13)-NH_2 and PWT2-[Dmt^1] in CHO cells stably expressing the NOP and classical opioid receptors and chimeric G proteins. Data are the mean ± S.E.M. for at least 4 separate experiments performed in duplicate.

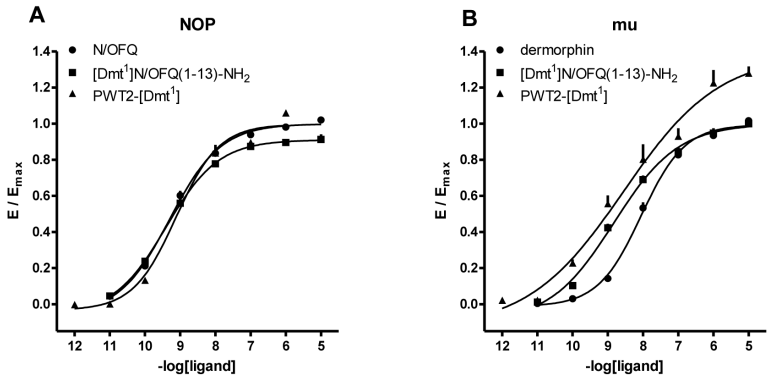

Figure 5.

Receptor / G protein interaction studies. Concentration response curves to standard agonists, [Dmt^1]N/OFQ(1-13)-NH_2 and PWT2-[Dmt^1] in CHO cells stably expressing the NOP/RLuc (panel A) or mu/RLuc (panel B) and the Gβ1/RGFP protein. Data are the mean ± S.E.M. for at least 3 separate experiments performed in duplicate.

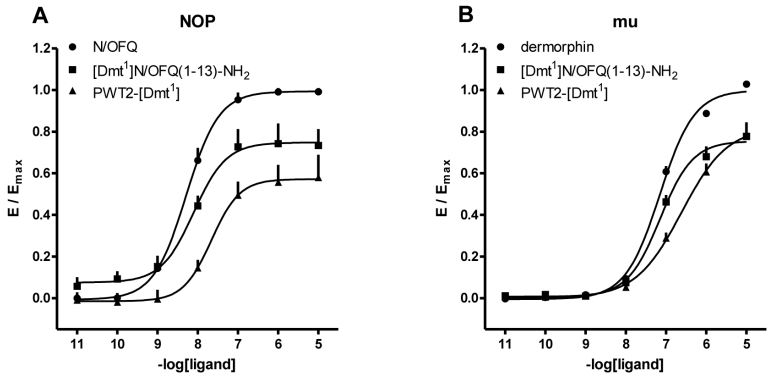

Figure 6.

Receptor / β-arrestin 2 interaction studies. Concentration response curves to N/OFQ, dermorphin, [Dmt^1]N/OFQ(1-13)-NH_2 and PWT2-[Dmt^1] in CHO cells stably expressing the NOP/RLuc (panel A) or mu/RLuc (panel B) and the β-arrestin 2/RGFP protein. Data are expressed as the mean ± S.E.M. for at least 4 separate experiments performed in duplicate.

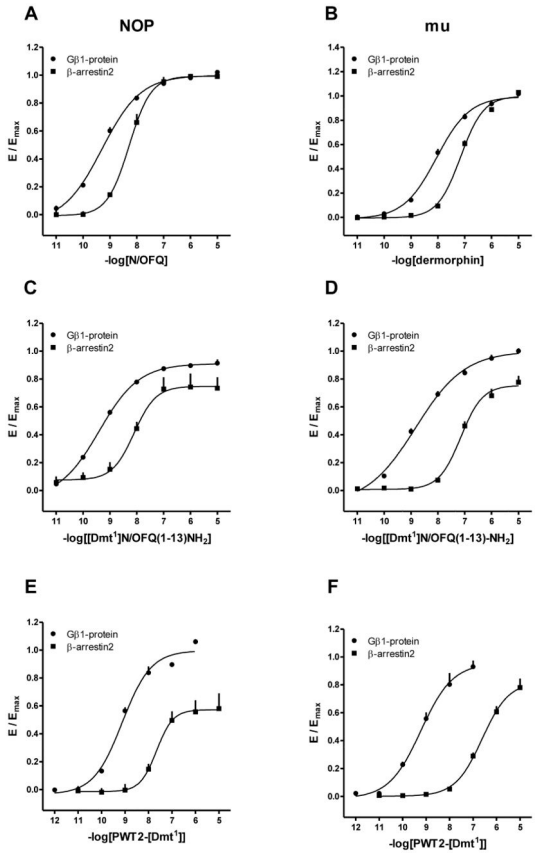

Figure 7.

BRET studies. Concentration response curves to N/OFQ, [Dmt^1]N/OFQ(1-13)-NH_2 and PWT2-[Dmt^1] (panel A, C and E) in cells stably expressing the NOP/RLuc and the Gβ1/RGFP or β-arrestin 2/RGFP proteins. Concentration response curves to dermorphin, [Dmt^1]N/OFQ(1-13)-NH_2 and PWT2-[Dmt^1] (panel B, D and F) in cells stably expressing the mu/RLuc and the Gβ1/RGFP or β-arrestin 2/RGFP proteins. Data are expressed as the mean ± S.E.M. for at least 4 separate experiments performed in duplicate.

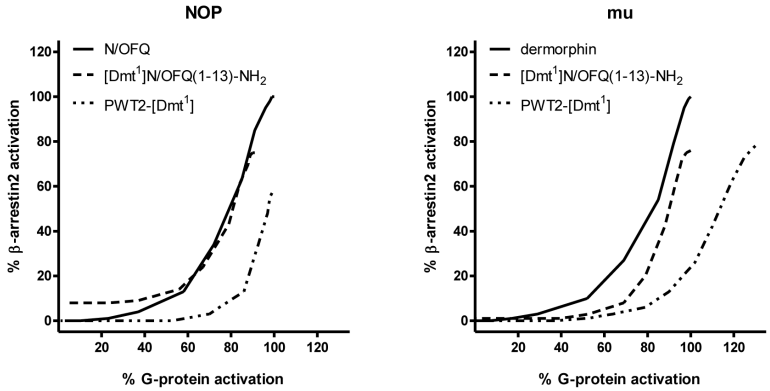

Figure 8.

Bias Plot showing the profile of [Dmt^1]N/OFQ(1-13)-NH_2 and PWT2-[Dmt^1] in comparison with the standard agonists N/OFQ for NOP (panel A) and dermorphin for mu (panel B).

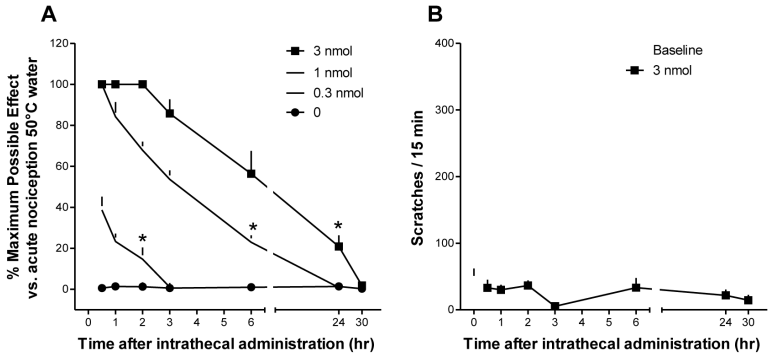

Figure 9.

Behavioural effects produced by intrathecal PWT2-[Dmt[1]]N/OFQ(1-13) in monkeys. **A**, percentage of maximum possible effect for antinociception measured by the warm water tail-withdrawal assay. **B**, scratching responses in a 15-min observation period after 3 nmol intrathecal of PWT2-[Dmt[1]]N/OFQ(1-13). Each data point represents the mean ± S.E.M. (n = 4). $*P < 0.05$, significantly different from vehicle from the first to the corresponding time point.

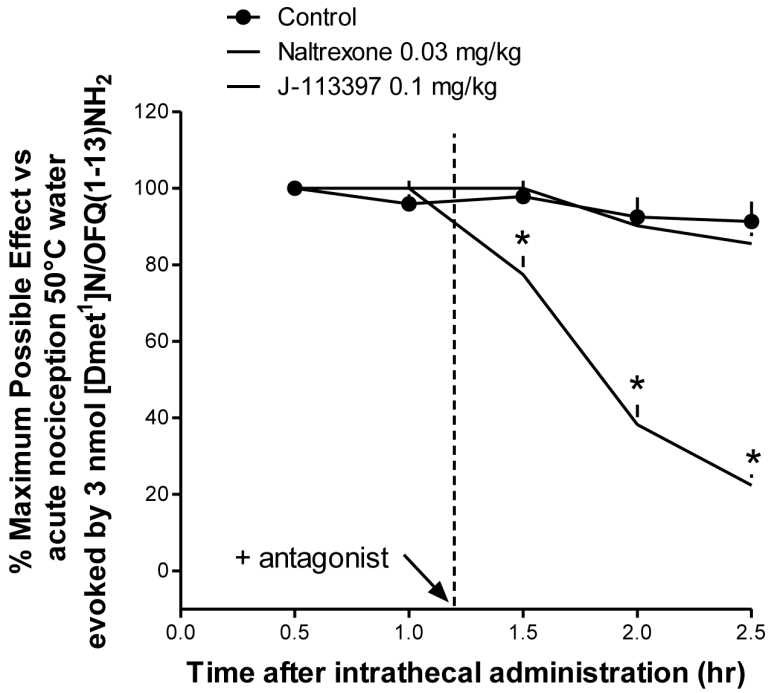

Figure 10.

Effects of antagonists on intrathecal PWT2-[Dmt[1]]N/OFQ(1-13) (3 nmol)-induced antinociception in monkeys. The antagonists naltrexone (0.03 mg/kg) or J-113397 (0.1 mg/kg) were given subcutaneously 10 min after the 1-hr time point. Percentage of maximum possible effect for antinociception measured by the warm water tail-withdrawal assay is shown. Each data point represents the mean ± S.E.M. (n = 4). *$P < 0.05$, significantly different from the vehicle condition.

Table 1

Displacement binding experiments. pK_i ($CL_{95\%}$) values of [Dmt^1]N/OFQ(1-13)-NH_2 and PWT2-[Dmt^1] in CHO cells expressing recombinant human NOP and classical opioid receptors.

	NOP	mu	kappa	delta
[Dmt^1]N/OFQ(1-13)-NH_2	10.39 (9.31-10.48)	10.04 (9.43-10.65)	10.38 (10.31-10.44)	9.99 (9.82-10.16)
PWT2-[Dmt^1]	9.13 (7.80-10.45)	9.25 (8.73-9.77)	9.13 (9.02-9.25)	8.42 (8.22-8.62)

N/OFQ, dermorphin, dynorphin A and DPDPE were used as standard ligands for the NOP, mu, kappa and delta receptors respectively.

Table 2

[^{35}S]GTPγS assay performed in CHO cells expressing recombinant human NOP and classical opioid receptors.

	NOP		mu		kappa		delta	
	pEC_{50} ($CL_{95\%}$)	α ± S.E.M.	pEC_{50} ($CL_{95\%}$)	α ± S.E.M.	pEC_{50} ($CL_{95\%}$)	α ± S.E.M.	pEC_{50} ($CL_{95\%}$)	α ± S.E.M.
[Dmt^{1}]N/OFQ(1-13)-NH_2	9.46 (9.20-9.72)	1.18 ± 0.16	8.58 (8.17-9.00)	1.10 ± 0.04	9.14 (9.43-8.86)	1.47 ± 0.17	8.17 (7.46-8.88)	1.09 ± 0.08
PWT2-[Dmt^{1}]	9.61 (9.36-9.86)	1.23 ± 0.13	8.51 (7.70-9.32)	0.98 ± 0.07	9.20 (8.94-9.45)	1.40 ± 0.11	8.16 (7.49-8.83)	0.87 ± 0.07

N/OFQ, dermorphin, dynorphin A and DPDPE were used as standard agonists for the NOP, mu, kappa, and delta receptors respectively.

Table 3

Effects of [Dmt^1]N/OFQ(1-13)-NH_2 and PWT2-[Dmt^1] at NOP and classical opioid receptors coupled with calcium signaling via chimeric G proteins.

	NOP		mu		kappa		delta	
	pEC_{50} ($CL_{95\%}$)	α ± S.E.M.	pEC_{50} ($CL_{95\%}$)	α ± S.E.M.	pEC_{50} ($CL_{95\%}$)	α ± S.E.M.	pEC_{50} ($CL_{95\%}$)	α ± S.E.M.
[Dmt^1]N/OFQ(1-13)-NH_2	9.18 (8.71-9.64)	0.99 ± 0.04	7.78 (7.14-8.42)	0.85 ± 0.04	7.66 (7.37-7.95)	0.92 ± 0.03	7.24 (6.92-7.57)	0.83 ± 0.07
PWT2-[Dmt^1]	7.83 (7.62-8.03)	0.98 ± 0.08	6.82 (6.20-7.43)	0.87 ± 0.04	6.40 (6.20-6.60)	0.86 ± 0.03	6.79 (6.42-7.16)	0.80 ± 0.08

N/OFQ, dermorphin, dynorphin A and DPDPE were used as standard agonists for calculating intrinsic activity at NOP, mu, kappa, and delta receptor respectively.

Table 4

Effects of standard agonists, [Dmt^1]N/OFQ(1-13)-NH_2 and PWT2-[Dmt^1] in promoting NOP/Gβ1 and mu/Gβ1 interaction.

	Gβ1-protein			
	NOP		mu	
	pEC_{50} ($CL_{95\%}$)	α ± S.E.M.	pEC_{50} ($CL_{95\%}$)	α ± S.E.M.
N/OFQ	9.30 (9.15-9.45)	1.00	crc incomplete	
Dermorphin	crc incomplete		8.03 (7.82-8.24)	1.00
[Dmt^1]N/OFQ(1-13)-NH_2	9.42 (9.15-9.69)	0.91 ± 0.02	8.80 (8.53-9.07)	0.99 ± 0.03
PWT2-[Dmt^1]	9.16 (8.86-9.46)	1.04 ± 0.04	8.82 (7.96-9.68)	1.43 ± 0.12

N/OFQ and dermorphin were used as reference agonists for calculating intrinsic activity at NOP and mu receptors, respectively. crc incomplete means that maximal effects could not be determined due to the low potency of the compounds.

Table 5

Effects of standard agonists, [Dmt^1]N/OFQ(1-13)-NH_2 and PWT2-[Dmt^1] in promoting NOP/β-arrestin2 and mu/ β-arrestin2 interactions.

	β-arrestin2			
	NOP		mu	
	pEC_{50} ($CL_{95\%}$)	α ± S.E.M.	pEC_{50} ($CL_{95\%}$)	α ± S.E.M.
N/OFQ	8.25 (7.99-8.52)	1.00	inactive	
Dermorphin	inactive		7.15 (7.05-7.25)	1.00
[Dmt^1]N/OFQ(1-13)-NH_2	8.15 (7.79-8.51)	0.75 ± 0.09	7.13 (7.07-7.19)	0.76 ± 0.05
PWT2-[Dmt^1]	7.67 (7.41-7.93)	0.58 ± 0.10	6.64 (6.50-6.78)	0.82 ± 0.07

N/OFQ and dermorphin were used as reference agonists for calculating intrinsic activity at NOP and mu receptors, respectively. Inactive means that the compound was inactive up to 1 μM.